

Non-adiabatic Storage of Short Light Pulses in an Atom–Cavity System

Tobias Macha,^{*} Eduardo Uruñuela, Wolfgang Alt, Maximilian Ammenwerth,

Deepak Pandey, Hannes Pfeifer, and Dieter Meschede

Institut für Angewandte Physik, Universität Bonn, Wegelerstraße 8, 53115 Bonn, Germany

We demonstrate the storage of 5 ns light pulses in an intrinsically fiber-coupled atomic memory. Our storage protocol addresses a regime beyond the conventional adiabatic limit, for which we extract the optimal control laser pulse properties from a numerical simulation of our system. We measure storage efficiencies of $(8.2 \pm 0.9) \%$, in close agreement with the maximum expected efficiency. Such well-controlled and high-bandwidth atom-photon interfaces are an attractive technology for future hybrid quantum networks.

Quantum networks are the basis for distributed quantum information processing [1, 2] and long-distance quantum communication [3, 4]. In these networks, distant nodes are connected via quantum channels, e.g. optical fibers guiding single photons as flying qubits [5]. The nodes for processing and storage of quantum information demand long coherence times and the ability to convert flying to stationary qubits (and vice versa). Atomic systems have shown to fulfill these criteria [6–8], but not for bandwidths beyond a few MHz as required for high-speed networking. This is a consequence of their naturally narrow transitions. Using collective effects, atomic vapor based implementations are able to store high-bandwidth pulses, but here the storage time is limited [9–11]. We overcome bandwidth limitations by modifying the properties of a single atom using a high-bandwidth, microscopic fiber Fabry-Pérot cavity (FFPC) [12]. A strong light-matter interaction, as required for the reversible storage of quantum information, is maintained due to the small cavity mode volume. Additionally, FFPCs offer an intrinsic fiber coupling that facilitates the implementation in networks.

In this Letter, we report on the Raman-assisted storage of a weak coherent input light pulse in a single atom coupled to a high-bandwidth optical resonator. In contrast to previously reported cavity experiments with a similar setting [13, 14], we apply two orders of magnitude shorter input pulses – even shorter than the atomic excited-state decay time constant $1/\gamma$. Prominent theoretical work [15–17] has been mostly concerned with realizing an adiabatic state transfer during the storage process and is not applicable in our case. Instead, we find an optimum pulse sequence in this fast storage regime by numerical simulations based on the full quantum-mechanical master equation describing our system. The ability to store high-bandwidth pulses makes our system a promising building block for hybrid quantum networks with solid-state platforms such as quantum dots [18].

Our photon memory consists of a single ^{87}Rb atom trapped at the center of a high-bandwidth FFPC. One of the fiber mirrors presents a higher transmission (HT), ensuring a highly directional input-output channel [19]. As depicted in Fig. 1a, the cavity is placed at the fo-

cus of four in-vacuum, aspheric lenses ($\text{NA} = 0.5$), which lead to a high beam pointing stability [20]. The lenses strongly focus two pairs of counter-propagating, red-detuned dipole trap beams at 860 nm which create a 2D optical lattice [21] in the xy -plane, see Fig. 1b. One of the lattices acts as a conveyor belt [22] to transport atoms from a magneto-optical trap (MOT) into the cavity. Confinement in the z -direction is provided by the intra-cavity, blue-detuned lock laser field at 770 nm, which is used for stabilizing the resonator length and for carrier-free Raman cooling in three dimensions [23, 24]. As a result, the atom is located with sub-wavelength precision at an antinode of the cavity mode driven by the input pulse. In particular, the mode is resonant to the Stark-shifted $|F = 2, m_F = -2\rangle \rightarrow |F' = 2, m_F = -1\rangle$ hyperfine transition of rubidium at 780 nm. The quantization axis is aligned with the cavity axis by applying a magnetic field of ~ 1.8 G.

In each experimental cycle, the memory is initialized by cooling and preparing the atom in the state $|F = 2, m_F = -2\rangle$ by optical pumping with an efficiency exceeding 95 %. As a first step of the storage protocol, we send a triggered, coherent input pulse with a mean photon number n and a duration of 5 ns (FWHM). It has a time-symmetric, sine-squared shaped probability amplitude $|\phi_{\text{in}}|$ of the electric field. When it enters through the HT mirror, a control laser pulse Ω in two-photon resonance is simultaneously applied from the side along the x -axis (Fig. 1b). This results in transferring the atom dominantly to the state $|F = 1, m_F = -1\rangle$, see Fig. 1c. After a storage time of $1 \mu\text{s}$, the photon is read out with an adiabatic control pulse to ensure maximum population transfer [25–27]. The cycle of state initialization, photon storage and retrieval is repeated with the same atom up to 1500 times for ~ 2 seconds, limited only by the efficiency of the currently employed cooling mechanism.

To find the optimum storage-assisting control laser pulse with time-dependent Rabi frequency $\Omega(t)$, we simulate the system based on a Lindblad master equation. The underlying Hamiltonian consists of the Jaynes-

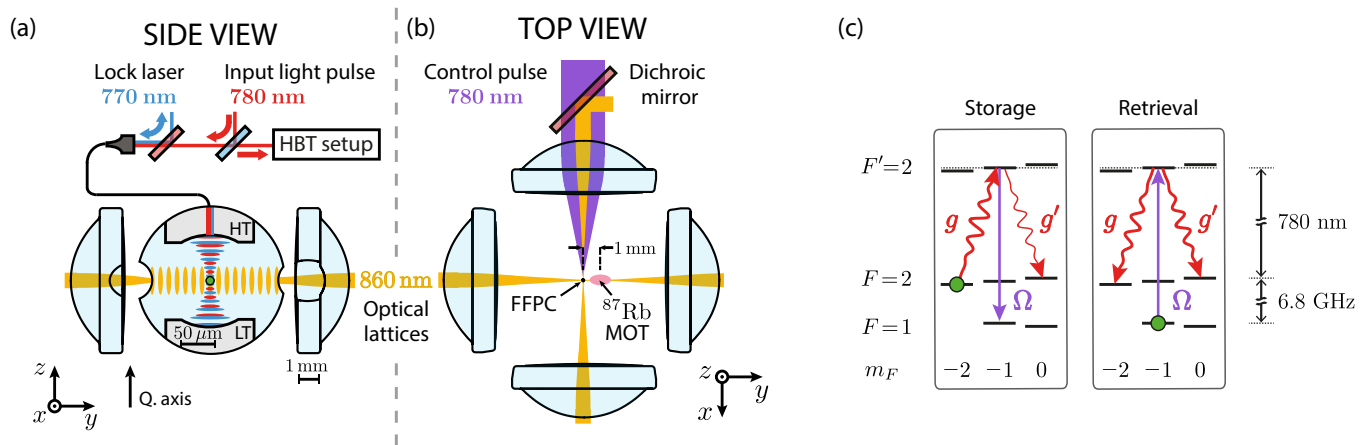


FIG. 1. Schematic side (a) and top (b) views of the experimental setup illustrate the optical lattices trapping a single rubidium (^{87}Rb) atom at the center of a microscopic fiber Fabry-Pérot cavity (FFPC). The high transmission (HT) mirror of the cavity is the access port for a coherent input light pulse, which is stored in the atomic memory via a control pulse entering from the side. Retrieved single photons are guided to a Hanbury-Brown and Twiss setup (HBT) for detection. (c) Photon storage for a cavity with two degenerate polarization modes. The first mode couples the initial state $|F, m_F\rangle = |2, -2\rangle$ to the excited state $|2', -1\rangle$ with a rate g and either results in coherent transfer to $|1, -1\rangle$ by the interaction with the control laser or in coherent leakage to $|2, 0\rangle$ via a second cavity mode with rate g' . The efficiency of an adiabatic retrieval process is not affected as the photon detection is polarization-insensitive.

Cummings Hamiltonian and additional driving terms

$$\hat{H}_d(t) = i\hbar \frac{\Omega(t)}{2} (\hat{\sigma}^\dagger - \hat{\sigma}) + \hbar \sqrt{2\kappa_{\text{HT}}} \cdot \sqrt{n} \cdot \phi_{\text{in}}(t) (\hat{a}^\dagger + \hat{a}) \quad (1)$$

where $\hat{\sigma}^\dagger, \hat{\sigma}$ are the flip operators of the atomic states that are coupled via $\Omega(t)$, while $\hat{a}^\dagger(\hat{a})$ is the creation (annihilation) operator of the driven cavity mode. The total cavity damping $\kappa = \kappa_{\text{HT}} + \kappa_{\text{loss}}$ is the sum of the pure transmission rate κ_{HT} , at which a coherent field ($\phi_{\text{in}}(t)$) impinging on the HT mirror interacts with the open system, and the undesired losses κ_{loss} , e.g. due to absorption and scattering in the mirrors.

Our cavity supports two degenerate polarization modes (σ^\pm), which couple two Zeeman states in the same hyperfine manifold $F = 2$ via an excited state (Fig. 1c). With the π -polarized control laser coupling the excited state to the $F = 1$ manifold, our choice of the initial Zeeman state leads to coherent dynamics in a tripod configuration [28]. We take this into account in our model by including two polarization cavity modes with effective atom-cavity coupling strengths g, g' and a total of four atomic states. The main effect of the ideally absent atom-cavity coupling g' is a coherent population leakage during a storage attempt. The photon storage efficiency η_{storage} , which is the transfer efficiency η_{transfer} from initial to target state normalized by the mean input photon number ($\eta_{\text{storage}} = \eta_{\text{transfer}}/n$), is thus decreased compared to a standard Lambda configuration [16].

In general, the storage efficiency depends crucially on the properties of the control pulse, being the temporal shape, the pulse amplitude, the detuning from the atomic

transition and the delay with respect to the input pulse. However, in a non-adiabatic regime we find that its exact temporal shape plays a minor role. A simple temporal compression of a pulse shape suitable for the adiabatic regime [17] is equally effective as a numerically optimized pulse shape for our short input pulse [29]. In case of zero single-photon detuning of the input pulse with respect to the atomic excited state, our simulation predicts the highest storage efficiency for a vanishing two-photon detuning of the Raman transition, as also predicted by [16]. The remaining pulse parameters for optimal storage are the peak Rabi frequency of the control laser and its delay τ_Ω .

Besides the pulse parameters, knowledge about the system parameters $g, g', \kappa_{\text{HT}}, \kappa_{\text{loss}}, \gamma$ is important for the storage process. κ_{HT} is known from the mirror characterization in [19] and $\kappa_{\text{loss}} = \kappa - \kappa_{\text{HT}}$ is obtained after measuring κ by probing the frequency-dependent cavity reflection. For determining g, g' , we take a measurement, during which we store an input pulse with on average $n = 2.1$ photons and reconstruct the retrieved pulse after the memory read-out, as shown in Fig. 2. A simulation-based fit of the resulting shape with g, g' as free parameters completes our set of system parameters: $(g, g', \kappa_{\text{HT}}, \kappa_{\text{loss}}, \gamma) = 2\pi \cdot (22, 27, 16, 25, 3)$ MHz.

Two additional measurements determine the coherent storage fraction. The first one omits the control pulse and thus indicates the incoherent state transfer due to optical pumping by the input pulse. The second measurement uses neither control nor input pulse, which indicates false state preparation. From the ratio of the integrated detection counts in Fig. 2, we obtain a coherent storage

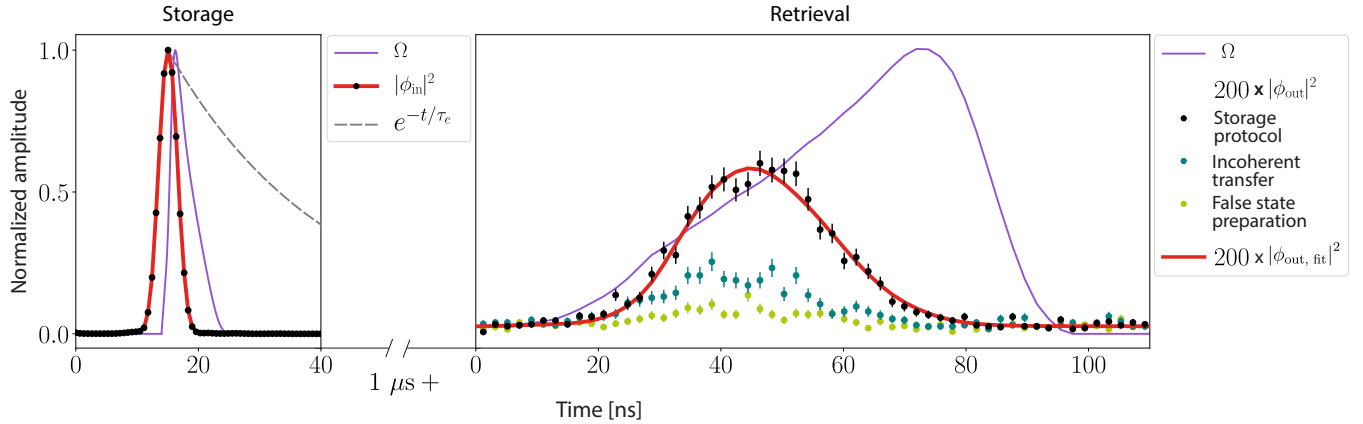


FIG. 2. On the left: The time-symmetric, sine-squared shaped input pulse with intensity probability amplitude $|\phi_{\text{in}}|^2$ (black points) sent to the HT mirror has a FWHM duration of 5 ns (red, solid line). For comparison, the atomic excited state decay with a time constant of $\tau_e = 26$ ns is shown (gray, dashed line). The control pulse with Rabi frequency Ω (purple, solid line) is applied with a delay of 4.4 ns with respect to the input pulse, in contrast to adiabatic storage protocols (see main text). All pulses are normalized to one. On the right: After a storage time of $1 \mu\text{s}$, a Raman control pulse Ω (gray, solid line) adiabatically generates a photon $|\phi_{\text{out}}|^2$ after the full storage protocol (black dots). By taking into account the incoherently transferred population in the absence of a control pulse (blue dots) and the counts due to false initial state preparation (green dots), we infer a coherent storage component of $(79 \pm 3) \%$. The data point values have been scaled by a factor of 200, while the Raman pulse is still normalized to one. From a simulation-based fit $|\phi_{\text{out, fit}}|^2$ (red, solid line) we extract the atom-cavity coupling strengths $(g, g') = 2\pi \cdot (22, 27)$ MHz.

component of $(79 \pm 3) \%$. In a Hanbury Brown-Twiss experiment we verify the single-photon character of the retrieved pulses by calculating the correlation function $g^{(2)}(0) = (12 \pm 6) \%$, which is consistent with the amount of background light and detector dark counts.

In a next step, the previously obtained system parameters are used to simulate the storage process in order to map out the full parameter space for the optimization of the storage efficiency η_{storage} . Here, η_{storage} is displayed as a function of the peak Rabi frequency of the control laser and its delay τ_{Ω} in Fig. 3a and the transfer efficiency η_{transfer} as a function the peak Rabi frequency and mean photon number per input pulse in Fig. 3b. The latter is of interest for cross-checking the photon number calibration, which is required to determine the storage efficiency per input photon.

The simulation results show efficiency revivals towards higher Rabi frequencies, which give insight into the underlying storage process. The revivals are a consequence of the excited state being significantly populated before it is mapped by the control laser to the target ground state in a coherent π -pulse interaction [16]. In contrast, a classic STIRAP [30] protocol does not show revivals. It relies on the adiabatic transfer between the ground states, which is no longer the most efficient storage method in the presented experiment.

We confirm the simulated behavior by measuring four independent parameter scans which are fitted to the two simulated maps simultaneously. To obtain the storage and transfer efficiencies from the measurement, the pho-

ton detection probabilities per storage attempt are corrected for the imperfect state preparation, the read-out efficiency of $(80 \pm 5) \%$, the transmission in the optical path and the detection efficiencies of $(19 \pm 7) \%$ and the spatial mode matching between fiber-guided and cavity mode of $(60 \pm 2) \%$ [19]. For an input pulse with $n = 1$ (see Fig. 3a) we observe a maximum, from which we deduce the storage efficiency of $\eta_{\text{storage}} = (8.2 \pm 0.9) \%$, which is close to the highest expected value of 9.7 % for our tripod system with cavity losses. Taking the aforementioned efficiencies into account, the end-to-end efficiency of creating an outgoing single-photon Fock state per impinging coherent state is $(0.9 \pm 0.1) \%$. For a larger number of photons per pulse (see Fig. 3b), we observe the expected saturation of the transfer efficiency. However, towards higher peak Rabi frequencies the results deviate from the simulation, which is more significant for higher mean photon numbers (Fig. 3a,b). We attribute this behavior to deviations in both the atom-cavity coupling strength and the ac Stark shift, which originate from variations of the atom position within the cavity mode and dipole traps. As a result, the optimum two-photon Rabi frequency is met at higher peak Rabi frequencies than expected.

With technical improvements such as the realization of a three-level (Lambda) configuration, the efficiency can already be improved by more than a factor of 2. Assuming negligible undesired cavity losses, storage efficiencies exceeding 40 % should be feasible with a single atom. The overall memory efficiency can be increased by fiber

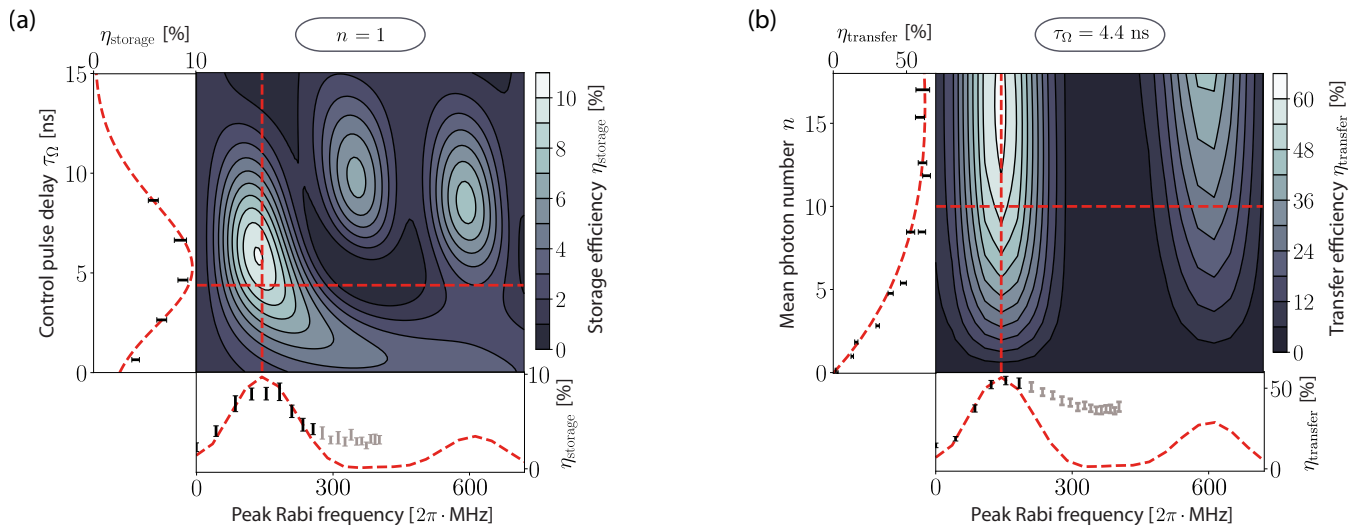


FIG. 3. Simulated efficiency maps and experimental pulse parameter scans. (a) For an input pulse containing a mean photon number of $n = 1$, the storage efficiency η_{storage} as a function of both control pulse peak Rabi frequency and control pulse delay τ_{Ω} is simulated. The non-adiabatic storage process reveals a significant atomic excited state population, which is then mapped by the control laser to the target ground state in a coherent π -pulse process. Thus, for higher peak Rabi frequencies efficiency revivals are observed. (b) For a fixed control pulse delay of 4.4 ns, the transfer efficiency η_{transfer} is simulated as a function of both control pulse peak Rabi frequency and mean photon number per pulse n . A simultaneous fit (red, dashed lines) of four independent, experimental parameter scans (black points) to the simulation of our system allows us to extract the storage efficiency $\eta_{\text{storage}} = (8.2 \pm 0.9) \%$ for a coherent input pulse with a mean photon number of $n = 1$.

cavities equipped with GRIN lenses [31], which reduce the losses due to a cavity-fiber mode-mismatch.

In conclusion, we have demonstrated the efficient, non-adiabatic storage of light pulses, which are, with 5 ns, much shorter than the atomic excited state lifetime of $\tau_e = 26$ ns. By simulating our atom-cavity system in dependence of its various parameters, we find the optimum control pulse for the highest possible photon storage efficiency and observe a remarkable agreement with experimentally obtained values.

Our system is capable of interacting with very short light pulses in a highly directional manner, thereby demonstrating functionality for a high-bandwidth quantum network. In the future, we will employ ensembles of atoms, which will lead to a further enhancement of light-matter interaction by collective effects [32], allowing for storage of even shorter pulses. In this way, true single-photon Fock states as provided by the emission of a quantum dot can interact with our system. Envisioning such a hybrid experiment, we have recently demonstrated that the quantum dot emission frequency can be stabilized to atomic transitions [33].

We acknowledge funding by the BMBF (Q.Link.X) and the Deutsche Forschungsgemeinschaft (SFB/TR 185 OS-CAR). We thank J. Gallego and E. Keiler for discussions and technical support in the early stage of the presented experiment.

* macha@iap.uni-bonn.de

- [1] P. Kok, W. J. Munro, K. Nemoto, T. C. Ralph, J. P. Dowling, and G. J. Milburn, *Rev. Mod. Phys.* **79**, 135 (2007).
- [2] J. I. Cirac, A. K. Ekert, S. F. Huelga, and C. Macchiavello, *Phys. Rev. A* **59**, 4249 (1999).
- [3] H. Briegel, W. Dür, J. I. Cirac, and P. Zoller, *Physical Review Letters* **81**, 5932 (1998).
- [4] L.-M. Duan, M. D. Lukin, J. I. Cirac, and P. Zoller, *Nature* **414**, 413 (2001).
- [5] T. E. Northup and R. Blatt, *Nature Photonics* **8**, 356 (2014).
- [6] M. Körber, O. Morin, S. Langenfeld, A. Neuzner, S. Ritter, and G. Rempe, *Nature Photonics* **12**, 18 (2018).
- [7] C. Langer, R. Ozeri, J. D. Jost, J. Chiaverini, B. DeMarco, A. Ben-Kish, R. B. Blakestad, J. Britton, D. B. Hume, W. M. Itano, D. Leibfried, R. Reichle, T. Rosenband, T. Schaetz, P. O. Schmidt, and D. J. Wineland, *Phys. Rev. Lett.* **95**, 060502 (2005).
- [8] O. Katz and O. Firstenberg, *Nature Communications* **9**, 2074 (2018).
- [9] J. Wolters, G. Buser, A. Horsley, L. Béguin, A. Jöckel, J. P. Jahn, R. J. Warburton, and P. Treutlein, *Physical Review Letters* **119**, 1 (2017).
- [10] N. Akopian, L. Wang, A. Rastelli, O. G. Schmidt, and V. Zwiller, *Nature Photonics* **5**, 2 (2011).
- [11] K. F. Reim, P. Michelberger, K. C. Lee, J. Nunn, N. K. Langford, and I. A. Walmsley, *Phys. Rev. Lett.* **107**, 053603 (2011).
- [12] D. Hunger, T. Steinmetz, Y. Colombe, C. Deutsch, T. W.

- Hänsch, and J. Reichel, *New Journal of Physics* **12**, 065038 (2010).
- [13] A. D. Boozer, A. Boca, R. Miller, T. E. Northup, and H. J. Kimble, *Physical Review Letters* **98**, 193601 (2007).
- [14] H. P. Specht, C. Nölleke, A. Reiserer, M. Uphoff, E. Figueroa, S. Ritter, and G. Rempe, *Nature* **473**, 190 (2011).
- [15] M. Fleischhauer, S. Yelin, and M. Lukin, *Optics Communications* **179**, 395 (2000).
- [16] A. V. Gorshkov, A. André, M. D. Lukin, and A. S. Sørensen, *Physical Review A* **76**, 033804 (2007).
- [17] J. Dille, P. Nisbet-Jones, B. W. Shore, and A. Kuhn, *Physical Review A* **85**, 023834 (2012).
- [18] R. Keil, M. Zopf, Y. Chen, B. Höfer, J. Zhang, F. Ding, and O. G. Schmidt, *Nature Communications* **8**, 15501 (2017).
- [19] J. Gallego, S. Ghosh, S. K. Alavi, W. Alt, M. Martinez-Dorantes, D. Meschede, and L. Ratschbacher, *Applied Physics B* **122**, 47 (2016).
- [20] M. Martinez-Dorantes, W. Alt, J. Gallego, S. Ghosh, L. Ratschbacher, Y. Völzke, and D. Meschede, *Physical Review Letters* **119**, 180503 (2017).
- [21] J. Gallego, W. Alt, T. Macha, M. Martinez-Dorantes, D. Pandey, and D. Meschede, *Physical Review Letters* **121**, 173603 (2018).
- [22] S. Kuhr, W. Alt, D. Schrader, M. Müller, V. Gomer, and D. Meschede, *Science* **293**, 278 (2001).
- [23] R. Reimann, W. Alt, T. Macha, D. Meschede, N. Thau, S. Yoon, and L. Ratschbacher, *New Journal of Physics* **16**, 113042 (2014).
- [24] A. Neuzner, S. Dürr, M. Körber, S. Ritter, and G. Rempe, *Physical Review A* **98**, 013401 (2018).
- [25] M. Mücke, J. Bochmann, C. Hahn, A. Neuzner, C. Nölleke, A. Reiserer, G. Rempe, and S. Ritter, *Physical Review A* **87**, 063805 (2013).
- [26] P. B. R. Nisbet-Jones, J. Dille, D. Ljunggren, and A. Kuhn, *New Journal of Physics* **13**, 103036 (2011).
- [27] M. Keller, B. Lange, K. Hayasaka, W. Lange, and H. Walther, *Nature* **431**, 1075 (2004).
- [28] N. V. Vitanov, A. A. Rangelov, B. W. Shore, and K. Bergmann, *Reviews of Modern Physics* **89**, 015006 (2017).
- [29] L. Giannelli, T. Schmit, T. Calarco, C. P. Koch, S. Ritter, and G. Morigi, *New Journal of Physics* **20**, 105009 (2018).
- [30] B. W. Shore, *Advances in Optics and Photonics* **9**, 563 (2017).
- [31] G. K. Gulati, H. Takahashi, N. Podoliak, P. Horak, and M. Keller, *Scientific Reports* **7**, 5556 (2017).
- [32] R. J. Thompson, G. Rempe, and H. J. Kimble, *Physical Review Letters* **68**, 1132 (1992).
- [33] M. Zopf, T. Macha, R. Keil, E. Uruñuela, Y. Chen, W. Alt, L. Ratschbacher, F. Ding, D. Meschede, and O. G. Schmidt, *Physical Review B* **98**, 161302(R) (2018).